



Digital Commons@

Loyola Marymount University
LMU Loyola Law School

Mechanical Engineering Faculty Works

Mechanical Engineering

8-2011

The Effect of Layer Orientation on the Mechanical Properties and Microstructure of a Polymer

V. Vega

J. Clements

T. Lam

A. Abad

B. Fritz

See next page for additional authors

Follow this and additional works at: https://digitalcommons.lmu.edu/mech_fac



Part of the [Mechanical Engineering Commons](#)

Digital Commons @ LMU & LLS Citation

Vega, V.; Clements, J.; Lam, T.; Abad, A.; Fritz, B.; Ula, N.; and Es-Said, Omar S., "The Effect of Layer Orientation on the Mechanical Properties and Microstructure of a Polymer" (2011). *Mechanical Engineering Faculty Works*. 14.

https://digitalcommons.lmu.edu/mech_fac/14

This Article is brought to you for free and open access by the Mechanical Engineering at Digital Commons @ Loyola Marymount University and Loyola Law School. It has been accepted for inclusion in Mechanical Engineering Faculty Works by an authorized administrator of Digital Commons@Loyola Marymount University and Loyola Law School. For more information, please contact digitalcommons@lmu.edu.

Authors

V. Vega, J. Clements, T. Lam, A. Abad, B. Fritz, N. Ula, and Omar S. Es-Said

The Effect of Layer Orientation on the Mechanical Properties and Microstructure of a Polymer

V. Vega, J. Clements, T. Lam, A. Abad, B. Fritz, N. Ula, and O.S. Es-Said

(Submitted June 15, 2010; in revised form July 18, 2010)

Rapid Prototyping (RP) is a method used everywhere from the entertainment industry to healthcare. Layer orientation is an important aspect of the final product. The objective of this research was to evaluate the effect of layer orientation on the mechanical strength and toughness of a polymer. The polymer used was a combination of two materials, ZP 130 and ZB 58, fused together in the Z Corporation Spectrum Z510 Rapid Prototyping Machine. ZP 130 is a powder composed of vinyl polymer (2-20%), sulfate salt (0-5%), and plaster that contains <1% crystalline silica (50-95%). ZB 58 is a liquid composed of glycerol (1-10%), preservative (sorbic acid salt) (0-2%), surfactant (<1%), pigment (<1%), and water (85-95%). After removal from the machine the samples were sealed with Z bond 101 which is Beta-methoxyethyl cyanoacrylate (60-100%). The layer orientations studied were the crack arrestor, crack divider, and short transverse with various combinations of the three, for a total of seven orientations. The mechanical strength was evaluated using tensile testing and three-point bend testing. The toughness was evaluated by Izod impact testing. Five samples for tensile testing and three-point bend testing as well as 15 samples for the Izod impact test for each of the seven orientations were made. The total number of samples was 175. The crack arrestor orientation was the strongest main orientation for the tensile and three-point bend test. Weibull analysis was done on the Izod impact testing due to high variation in the results for the crack arrestor and short transverse directions. It was found that the layer orientation and surface roughness played a significant role in the penetration of the Z bond 101 coating and in the overall strength of the samples.

Keywords 3D printing, fused deposition machine, layer orientation, mechanical strength, polymers, rapid prototyping, toughness

1. Introduction

Rapid Prototyping (RP) is used to help visualize concepts or models as well as prototyped parts. One of the methods of producing an RP specimen is a 3-D printer. It is a favored method because it is inexpensive, fast and uses very little material. The strength of the RP specimen is based on two factors, the material that the specimen is made of, and the orientation of the RP layers. The orientation of the specimen layout in the 3-D printer is examined in this study.

The samples in this study were made using the Spectrum Z510 Full Color System. It produces high-definition, full-color prototypes quickly and affordably by using inkjet printing. The samples were created from ZP™ 130 powder, which is composed of vinyl polymer (2-20%), sulfate salt (0-5%), and plaster that contains <1% crystalline silica (50-95%). This is

then solidified by ZP™ 58 which is a liquid composed of glycerol (1-10%), preservative (sorbic acid salt) (0-2%), surfactant (<1%), pigment (<1%), and water (85-95%). Finally, the samples are coated with Z-Bond™ 101 medium strength cyanoacrylate which is Beta-methoxyethyl cyanoacrylate (60-100%) (Ref 1-3).

The main orientations examined were termed the crack arrestor (A), crack divider (D), and short transverse (T) (Fig. 1) (Ref 4). Several other orientations that were a combination of the A, D, and T orientations were also examined.

It was reported by Embury et al. (Ref 4) that in the crack arrestor orientation each layer acts as a road block to total fracture. The crack must first break a layer and start again on a subsequent layer until final fracture. In the crack divider orientation, the initial crack is divided into multiple smaller cracks that then have to continue through the remaining specimen and all layers. Es-Said et al. data (Ref 5) agrees with Embury et al. (Ref 4) on the crack arrestor orientation. They (Ref 5) also found that the short transverse direction to be much weaker than the crack arrestor because the crack is perpendicular to the applied stress and advances with little resistance between the deposited layers. The layers in this orientation are parallel to the long transverse direction which is the same direction of the propagation of the crack.

Es-Said et al. (Ref 5) results revealed that the fracture paths were controlled by either weak interlayer bonding or interlayer porosity. In the tensile testing, the weak interlayer bonding was a result of residual stresses caused by shrinkage or by the low molecular diffusion and low cross-linking between the polymer layers during deposition from the melt. The interlayer porosity reduced the load-bearing area across the layers and hence

V. Vega, A. Abad, and B. Fritz, Northrop Grumman Corporation, Aerospace Systems Sector, One Hornet Way, El Segundo, CA 90425; J. Clements, T. Lam, and O.S. Es-Said, Mechanical Engineering Department, Loyola Marymount University, Los Angeles, CA 90045-8145; and N. Ula, Electrical Engineering Department, Loyola Marymount University, Los Angeles, CA 90045-8145. Contact e-mail: oessaid@lmu.edu.

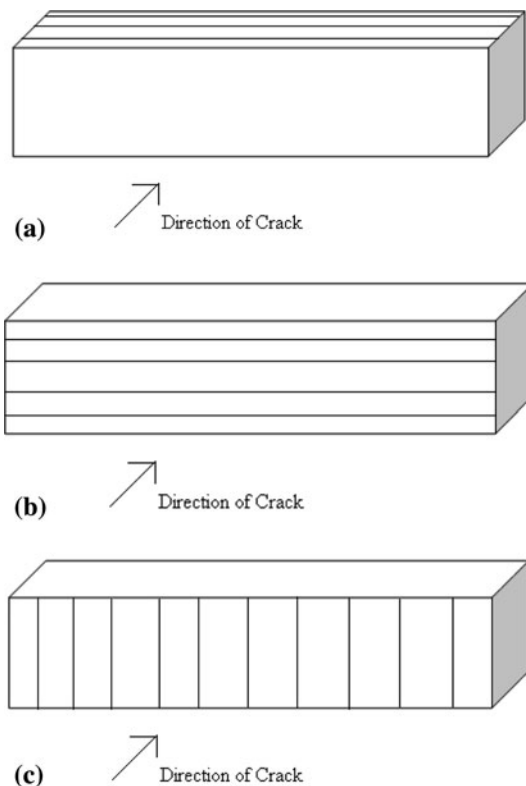


Fig. 1 Schematic diagram of the sample orientations (Ref 4). (a) Crack arrestor, (b) crack divider, and (c) short transverse

provided an easy fracture path. The pores were mainly located between the 2-D layers of the samples thus they could be easily separated by interfacial shear loads. They (Ref 5) also found through three-point bend testing that flexure testing induces shear stresses in the test samples. This can cause the low strength interfaces between the 2-D layers to delaminate prior to fracture. Finally, through Izod impact testing, it was found that weak interfaces that are parallel to the crack front provide an easy path for crack propagation and absorb the lowest amount of energy.

It was expected based on the results from the previous works on the ABS P400 polymers (Ref 5) that the A and D orientations would be the strongest with the T orientation being the weakest. There were no expectations on the combination orientations. The objective of this research was to evaluate the effect of the layer orientations: A, D, T and their combinations on the mechanical strength and toughness of rapid prototype samples of ZP 130 combined with ZB58.

2. Materials and Testing

Table 1 shows the composition of ZP™ 130 Powder (Ref 1). This powder is fused together in the Z Corporation Spectrum Z510 Rapid Prototyping Machine using the ZP™ 58 Binder whose components are shown in Table 2 (Ref 2). Once the samples have been prepared in the Z510 RP Machine they experience a rapid polymerization through the application of the Z-Bond™ 101 medium strength Cryanoacrylate. The composition of the Z-Bond™ 101 medium strength Cryanoacrylate is shown in Table 3 (Ref 3).

Table 1 ZP™ 130 powder composition (Ref 1)

Component classified as dangerous (CHIP3)	Approximate % by weight
1. Plaster which contains crystalline silica(a) at <1%	50-95
2. Vinyl polymer	2-20
3. Sulfate salt	0-5

(a) There is <0.1% respirable crystalline silica, no anticipated OSHA/TLV overexposure expected

Table 2 ZP™ 58 binder composition (Ref 2)

Components	Approximate % by weight
1. Glycerol	1-10
2. Preservative (Sorbic acid salt)	0-2
3. Surfactant	<1
4. Pigment	<20
5. Water	85-95

Table 3 Z-Bond™ 101 medium strength cryanoacrylate composition (Ref 3)

Hazardous components	%
Beta-methoxyethyl cyanoacrylate	60-100

To generate the samples, CAD drawings were created and submitted to be printed. The printer system rolls out a layer ZP™ 130 powder, then an inkjet printer deposits ZP™ 58 binder which solidifies the cross-section of the piece. Next the position of the part is lowered and a new layer of the ZP™ 130 powder is rolled over the semi-solidified piece and another layer is printed. This process is repeated until the sample is generated. The completed sample from the machine is very weak until the final step of applying Z-Bond™ 101 medium strength is accomplished, which improves the sample strength. Seven orientations were created. These are the arrestor (A), the divider (D), and the short transverse (T), AD, AT, DT (all with 50% of each orientation), and ADT (with 33% of each orientation). Five samples of tensile and three-point bend samples and 15 samples of Charpy Impact testing were generated for the seven orientations. The total number of samples was 175. A schematic of the Spectrum Z510 Full Color System and its process to make the part is shown in Fig. 2 (Ref 6).

Tensile testing and three-point bend testing were performed using an Instron 4505 machine. Izod testing was performed using an impact test machine, Custom Scientific Instruments, Inc., model CS-137. The dimension specifications for each test are shown in Fig. 3. Optical microscopy was performed at 6× magnification using a Wesco microscope, Indu Vu 5000 series. The surface of the fractured samples were examined and characterized using a JEOL JSM-6400 Scanning Electron Microscope (SEM). Secondary electron imaging of the fracture surfaces was carried out at 15 kV, about 30 mm working distance, the beam current was approximately 1 nA.



Fig. 2 Diagram of how the Spectrum Z510 Full Color System works (Ref 5)

3. Results

The average values for all the mechanical strength and toughness data of the sample orientations through all of the tests are shown in Fig. 4-6.

3.1 Main Orientations

The tensile data of the samples are shown in Table 4. The average stress was the highest for the sample in the A orientation with a stress value of 8.7 Pa (1.26 ksi). This was followed by the D then T orientations with a stress of 7.7 and 5.9 Pa (1.11 and 0.85 ksi), respectively. The standard deviations for these samples were 0.11, 0.05, and 0.03, respectively.

The three-point bend test data are shown in Table 5. For three-point bend testing the modulus of rupture (MOR) is calculated as a function of the applied force, length between rollers of the test setup and the width and thickness of the specimen. The average MOR was the highest for the samples in the A and T orientations with 27.2 and 21.8 Pa (3.94 and 3.17 ksi), respectively. These were followed by the D direction with a MOR value of 19.8 Pa (2.87 ksi). The standard deviations for these samples were 0.36, 0.14, and 0.07, respectively.

This is in accord with the results of Es-Said et al. (Ref 5) for both tensile testing and three-point bend testing. The A samples (0° in their designation) was consistently higher than the T (90° in their designation). The percent difference in the tensile strength and three-point bending strength in their case was 55 and 56%, respectively. In this work, the percent difference is 32 and 20%. This is due to the difference in the deposited materials and consequently in the microstructures. Es-Said et al. used an ABS P400 plastic and a fused deposition modeling (FDM) machine which works on an “additive” principle in which layers are placed on top of one another from an extrusion nozzle, whereas this study uses a 3-D print method that prints a liquid over a powder to solidify it layer by layer. The major difference is the coating used in this study. In Es-Said et al. (Ref 5), they were able to remove their generated sample from the machine and begin testing, whereas this study required the

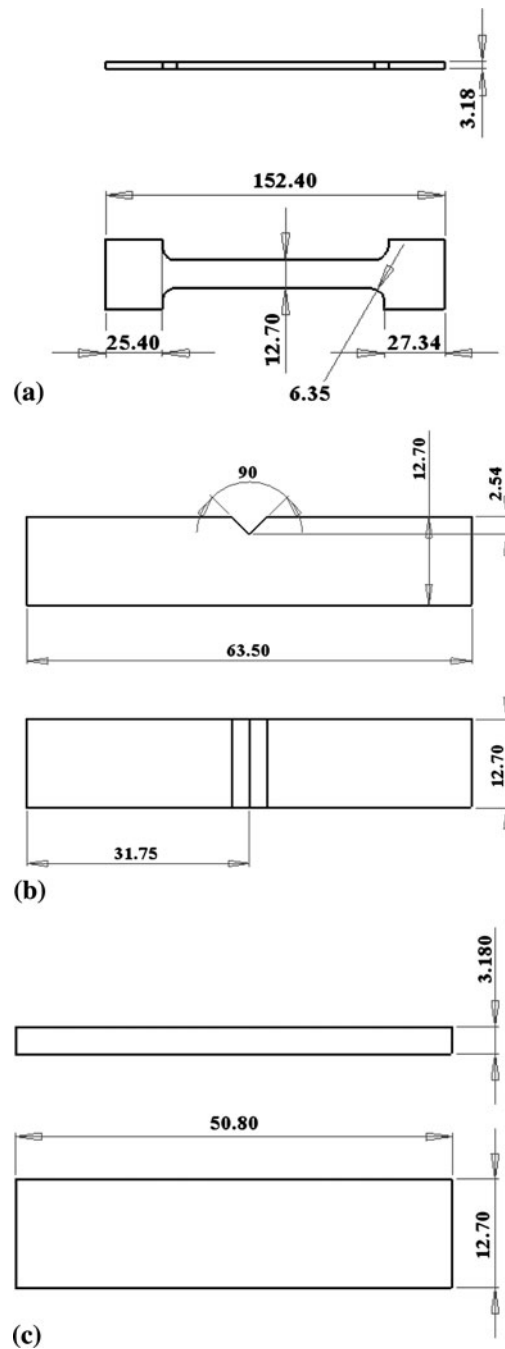


Fig. 3 Test sample dimensions (mm). (a) Tensile test sample dimensions, (b) Izod impact energy test sample dimensions, and (c) three-point bend test sample dimensions

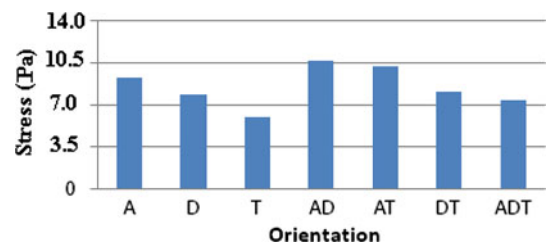


Fig. 4 Average stress values for tensile testing (Pa)

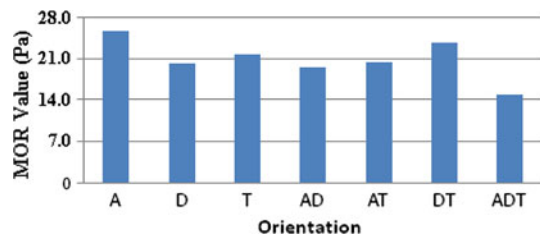


Fig. 5 Average MOR values for three-point bend testing (Pa)

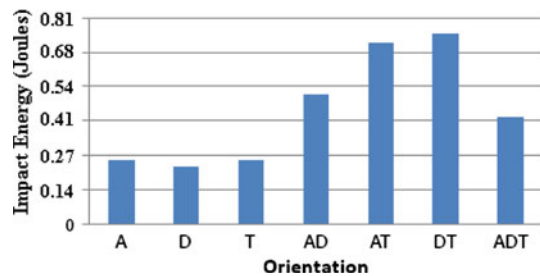


Fig. 6 Average impact energy values for Izod impact testing (J)

Table 4 Tensile test results

Sample	Stress, Pa	Stress, ksi
A1	9.19	1.33
A2	8.54	1.24
A3	10.45	1.52
A4	9.49	1.38
A5	7.66	1.11
D1	7.93	1.15
D2	7.37	1.07
D3	7.21	1.05
D4	8.18	1.19
D5	7.68	1.11
T1	5.81	0.84
T2	5.72	0.83
T3	5.77	0.84
T4	6.33	0.92
T5	5.73	0.83
AT1	9.75	1.42
AT2	9.16	1.33
AT3	11.03	1.60
AT4	9.67	1.40
AT5	10.73	1.56
AD1	10.23	1.49
AD2	10.77	1.56
AD3	10.95	1.59
AD4	10.39	1.51
AD5	10.24	1.49
DT1	6.39	0.93
DT2	7.97	1.16
DT3	7.52	1.09
DT4	9.56	1.39
DT5	8.03	1.17
ADT1	5.62	0.82
ADT2	8.98	1.30
ADT3	7.89	1.15
ADT4	6.13	0.89
ADT5	7.64	1.11

Table 5 Three-point bend test results

Sample	Stress, Pa	Stress, ksi
A1	29.92	4.34
A2	22.14	3.21
A3	26.62	3.86
A4	22.96	3.33
A5	24.94	3.62
D1	14.91	2.16
D2	21.97	3.19
D3	18.39	2.67
D4	22.67	3.29
D5	20.79	3.02
T1	22.59	3.28
T2	20.31	2.95
T3	19.32	2.80
T4	25.22	3.66
T5	19.83	2.88
AT1	18.67	2.71
AT2	16.79	2.44
AT3	15.64	2.27
AT4	24.80	3.60
AT5	24.63	3.58
AD1	21.47	3.12
AD2	20.39	2.96
AD3	18.94	2.75
AD4	16.84	2.44
AD5	18.38	2.67
DT1	18.71	2.72
DT2	24.98	3.63
DT3	26.46	3.84
DT4	24.16	3.51
DT5	22.45	3.26
ADT1	14.59	2.12
ADT2	12.73	1.85
ADT3	14.49	2.10
ADT4	15.40	2.24
ADT5	16.38	2.38

sample to be coated and let cure for several hours. This coating causes rapid polymerization where it was able to penetrate and essentially fuse together the layers of the sample, especially around the edges.

The Izod test results for the A and D orientations had lots of scattered data in the original five samples tested. Thus, 10 more samples were created from the same RP batch for the A, D, and T orientations. These results are shown in Table 6. The highest average energy absorbed for the Izod testing was the A and T orientations. The A and T orientations had an impact energy of 0.25 J (0.18 ft-lbs) with a standard deviation of 0.06 followed by the D orientation with 0.23 J (0.17 ft-lbs) and standard deviation of 0.014.

The Weibull Modulus was calculated for the Izod test samples to investigate the variability of the results. This was accomplished using the following formula:

$$F(V_o) = 1 - P(V_o) = 1 - \exp\left[-\frac{\sigma - \sigma_o^m}{\sigma_o^m}\right], \quad (\text{Eq } 1)$$

where $F(V_o)$ is the probability of failure, $P(V_o)$ is the probability of success, σ is the applied stress, σ_u is the stress level below which the probability of failure is zero, σ_o is the average strength, and m is the Weibull Modulus (Ref 7).

The Weibull Modulus, m , for A, D, and T were 3.3, 15.9, and 4.3, respectively. The low Weibull modulus number for the

Table 6 Izod impact test results

Sample	Impact energy, J	Impact energy, ft-lbs
A1	0.16	0.12
A2	0.35	0.26
A3	0.19	0.14
A4	0.18	0.13
A5	0.22	0.16
A6	0.22	0.16
A7	0.23	0.17
A8	0.20	0.15
A9	0.22	0.16
A10	0.28	0.21
A11	0.52	0.38
A12	0.23	0.17
A13	0.34	0.25
A14	0.22	0.16
A15	0.24	0.18
D1	0.20	0.15
D2	0.21	0.16
D3	0.20	0.15
D4	0.20	0.15
D5	0.20	0.15
D6	0.24	0.18
D7	0.23	0.17
D8	0.23	0.17
D9	0.22	0.16
D10	0.20	0.15
D11	0.24	0.18
D12	0.26	0.19
D13	0.23	0.17
D14	0.26	0.19
D15	0.23	0.17
T1	0.21	0.16
T2	0.20	0.15
T3	0.20	0.15
T4	0.39	0.29
T5	0.47	0.35
T6	0.22	0.16
T7	0.24	0.18
T8	0.22	0.16
T9	0.22	0.16
T10	0.28	0.21
T11	0.22	0.16
T12	0.20	0.15
T13	0.24	0.18
T14	0.23	0.17
T15	0.23	0.17
AD1	0.54	0.40
AD2	0.24	0.18
AD3	0.16	0.12
AD4	1.00	0.74
AD5	0.60	0.44
AT1	0.56	0.42
AT2	0.68	0.50
AT3	0.99	0.73
AT4	0.81	0.60
AT5	0.53	0.39
DT1	0.69	0.51
DT2	0.75	0.55
DT3	0.81	0.60
DT4	0.75	0.55
DT5	0.76	0.56
ADT1	0.15	0.11
ADT2	0.20	0.15
ADT3	0.20	0.15
ADT4	0.72	0.53
ADT5	0.83	0.61

A and T orientations reveal a low slope for this data and results in a higher variation of data than the D orientation which had a high Weibull Modulus number showing that there was a large slope with much less variation.

3.2 Combined Orientations

The tensile data for the combined samples revealed that the sample orientations of AD and AT were the strongest with a stress of 10.3 and 10.1 Pa (1.5 and 1.46 ksi) with standard deviations of 0.04 and 0.11, respectively. These values are higher than the strongest main orientation, A, by >13%.

However, in the three-point bend test the strongest combined orientations were DT and AT with MOR values of 24.1 and 22.7 Pa (3.5 and 3.29 ksi) with standard deviations of 0.24 and 0.5, respectively. These values are lower than the strongest main orientation, A, by >9%.

The Izod impact test results agreed with the three-point bend test in that DT and AT were the toughest with impact energy values of 0.75 and 0.71 J (0.55 and 0.52 ft-lbs) with standard deviation of 0.03 and 0.14, respectively. All of the combination orientation impact energy values for the Izod test were higher than the main orientations. The weakest combination was the ADT orientation, with a value of 0.42 J (0.31 ft-lbs), and a standard deviation of 0.24 which is 39% higher than the highest main orientations, A and T.

3.3 Tensile Samples with Rough Surfaces

It was found during the generation of the samples that one batch of tensile samples in the A orientation from the Z510 Rapid Prototyping Machine had very smooth surfaces compared to other batches, especially once they were coated. These eight smooth samples were coated and compared to 10 rough samples, five of which were from the original set. These samples were tested and the results are shown in Table 7.

The smooth samples were more than 40% weaker than the samples that had a rougher surface. The strongest smooth sample had a stress of 6.87 Pa (0.99 ksi), while the weakest rough surface sample had a stress of 7.67 Pa (1.11 ksi).

Table 7 Rough vs. smooth tensile sample results

Surface condition	Sample	Stress, Pa	Stress, ksi
Rough	A1	9.20	1.33
Rough	A2	8.55	1.24
Rough	A3	10.45	1.52
Rough	A4	9.50	1.38
Rough	A5	7.67	1.11
Rough	A7T	10.65	1.55
Rough	A8T	13.99	2.03
Rough	A9T	14.30	2.07
Rough	A10T	7.78	1.13
Smooth	A8	5.25	0.76
Smooth	A9	5.25	0.76
Smooth	A10	6.13	0.89
Smooth	A11	6.87	1.00
Smooth	A12	6.20	0.90
Smooth	A13	5.72	0.83
Smooth	A14	6.62	0.96
Smooth	A15	5.67	0.82

4. Discussion

The fractured tensile and Izod samples are shown in Fig. 7-12(a). The optical microscope images and SEM fractographs of the fractured surfaces are shown in Fig. 7-12(b, c), respectively. The optical microscope images at $6\times$ magnification show the interior parts of the samples (powder with different layer orientations) where the coating did not achieve full penetration. The A and D orientations, Fig. 7 and 8(b) and especially Fig. 10 and 11(b), show a very rough surface of the interior powder, alluding to the resistance of the material to cracking. The T orientation, Fig. 9(b) and especially Fig. 12(b), shows the interior powder to be very flat, indicating that there was little to no resistance to cracking. However, the strength and toughness effect of the layer orientation of the powder

materials of the samples in this study plays a minor role compared to the strength and toughness effect of the coating.

The SEM fractographs reveal that the coatings on all of the samples are similar regardless of the layer orientation, Fig. 7-12(c). This is because the coating causes the sample to experience rapid polymerization. Once the coating is applied the sample fuses together forming one solid bonded piece. In other words, the coating obscures the orientation of the powder material in the images shown in Fig. 7-12(c). It is from this coating that the samples gain the majority of their strength and toughness depending on the penetration into the layers.

The tensile and three-point bend results of this study are qualitatively in accord with the results of Es-Said et al. (Ref 5), however, for the three-point bending and Izod impact energy, the results were different. This is due to the different materials

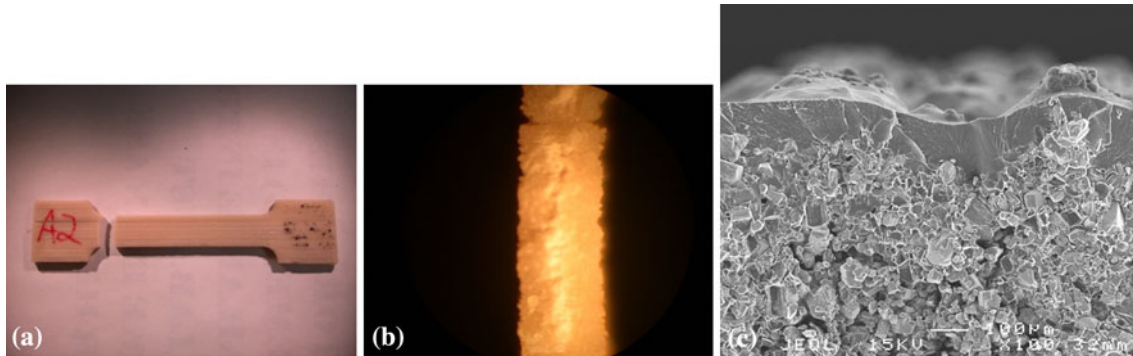


Fig. 7 Photo documentation of the crack arrestor (A) after tensile testing

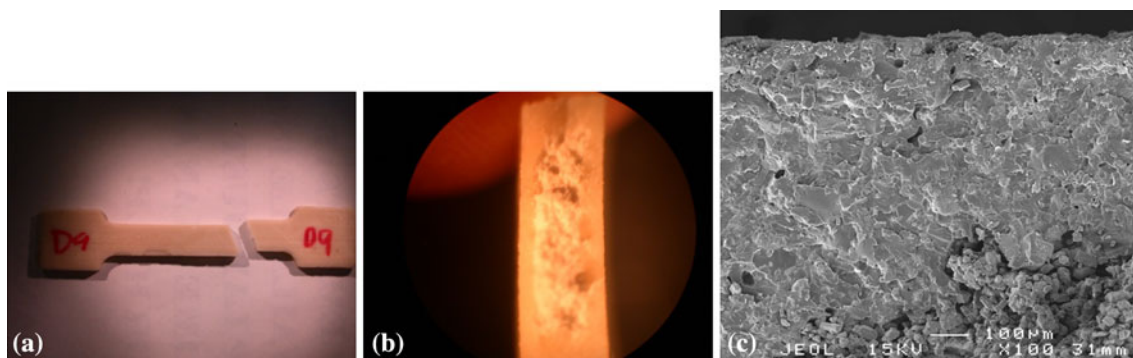


Fig. 8 Photo documentation of the crack divider (D) after tensile testing

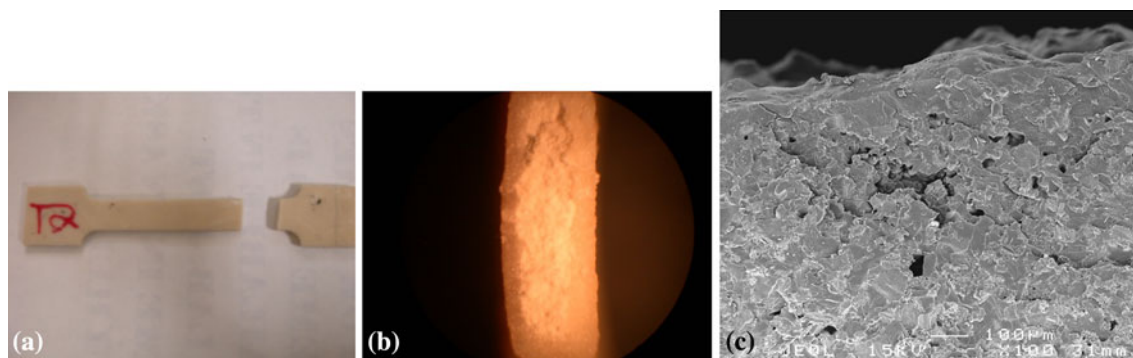


Fig. 9 Photo documentation of the short transverse (T) after tensile testing

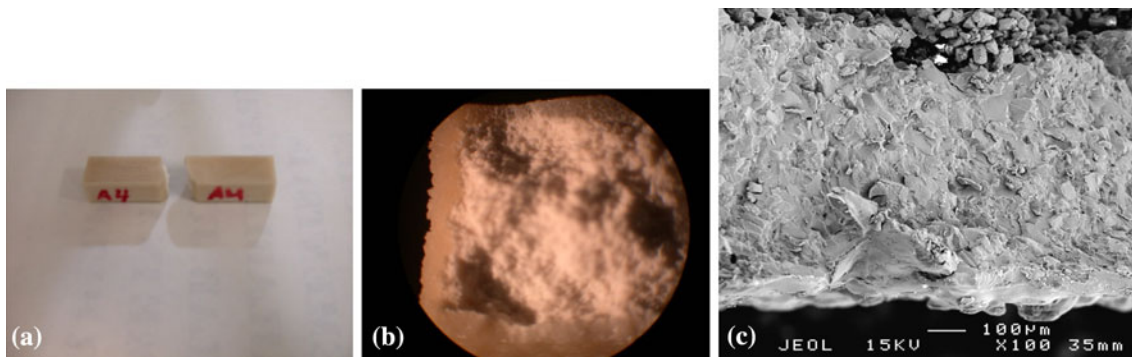


Fig. 10 Photo documentation of the crack arrester (A) after Izod impact testing

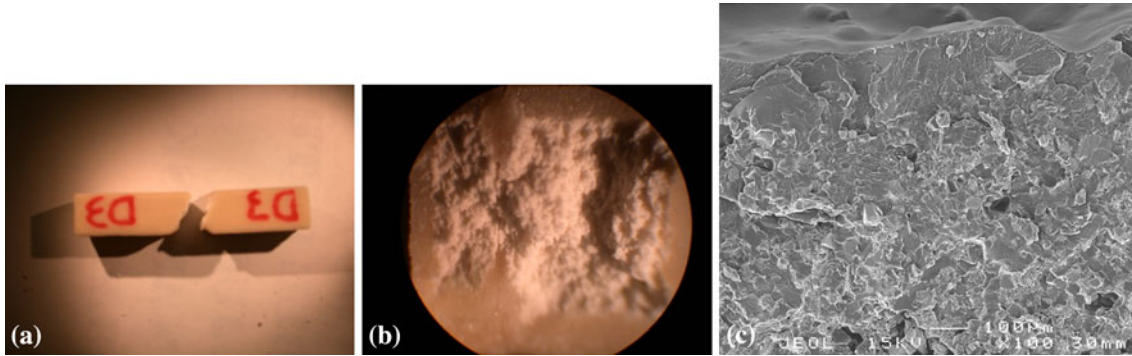


Fig. 11 Photo documentation of the crack divider (D) after Izod impact testing

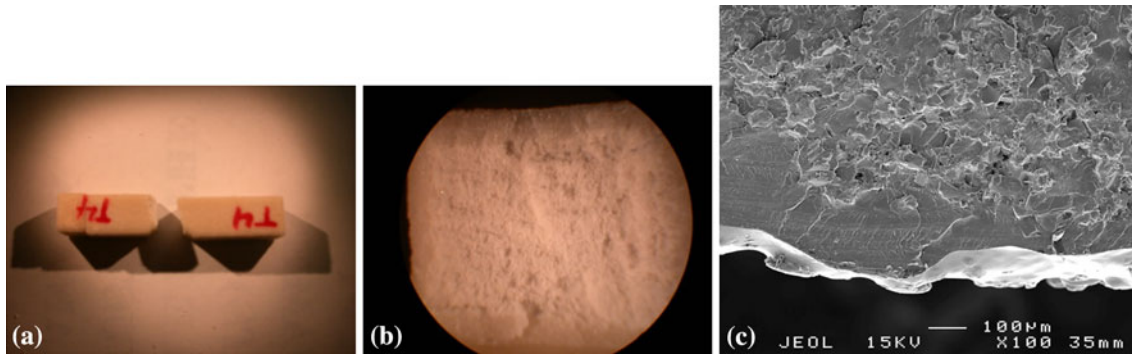


Fig. 12 Photo documentation of the Short Transverse (T) after Izod impact testing

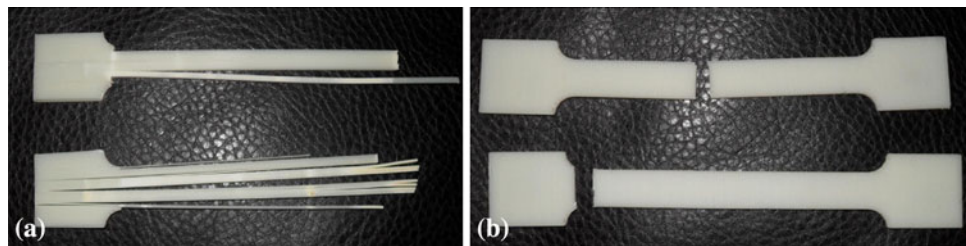


Fig. 13 Tensile test samples from Es-Said et al. (a) arrester/0° and (b) transverse/90°

and processes used to create the test samples. Es-Said et al. used an ABS plastic and a FDM machine. When broken, the 0° orientation shows fracture by individual layers and the 90° orientation shows a clean break through layers which are

visible by the naked eye. The tensile test, three-point bend test and Izod test samples from Es-Said et al. (Ref 5) are shown in Fig. 13-15. Also, no coating was applied to the samples (Ref 5). In this study, a 3-D print method was used and the

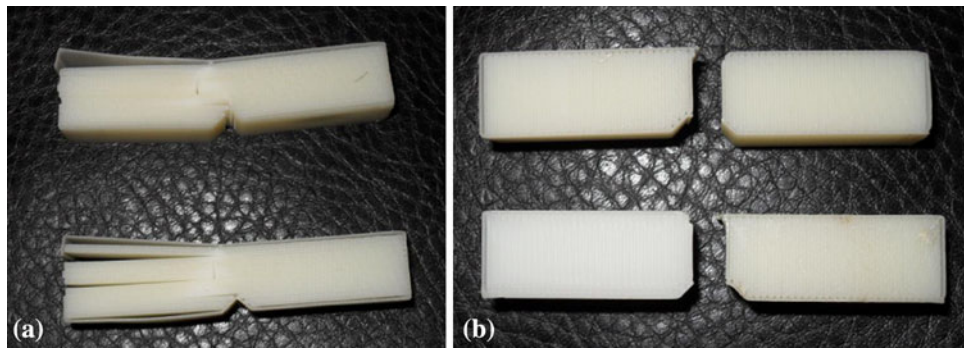


Fig. 14 Izod impact test samples from Es-Said et al. (a) arrestor/0° and (b) transverse/90°

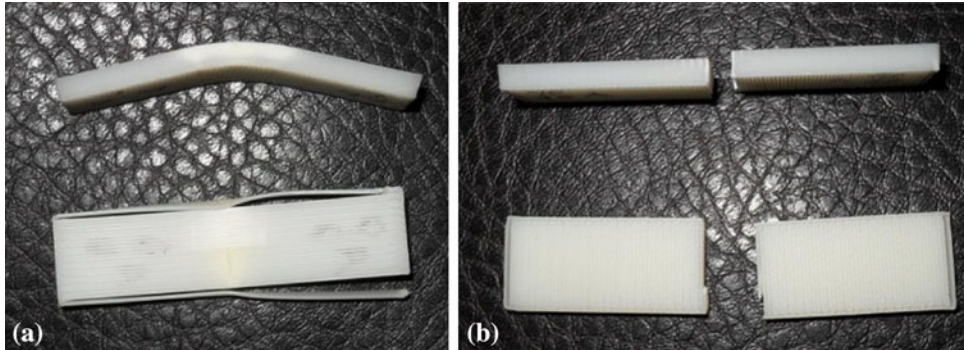


Fig. 15 Three-point bend test samples from Es-Said et al. (a) arrestor/0° and (b) transverse/90°

samples were coated on completion to cure the samples and give them handling strength.

In this study, it was found that the layer orientation of the sample was the enabler of the level of penetration that the coating was able to reach for each sample. For the tensile test, the results were as expected with the A orientation being the strongest and the T orientation being weaker. However, the results were not as drastic as they were in Es-Said et al. (Ref 5). This again is due to the penetration of the coating. The A and D orientations had the coating running the length of the sample, meaning that there was long continuous coating that had to be broken for final fracture. The T orientation, however, had a strong bond between each layer along the outside of the sample, meaning that there were multiple coatings along the sample that were experiencing the load before final fracture. This is shown in Fig. 16.

In the Izod test, the A orientation layers ran in such a manner as to prohibit the coating from penetrating the sample, especially at the crack origin. The T orientation layers, however, ran parallel to the crack so that the coating was able to penetrate even further into to sample at the point of impact, Fig. 17(a-c). That is why the A and T orientations had higher values than the D orientation, Fig. 6.

This is also the case in the three-point bend samples. It was found that the A orientation was the strongest, but that the T orientation was much stronger than the D orientation. Examining the schematic of the coating penetration for the three-point bend samples, Fig. 18(a-c), it is shown that the A and T orientations have more coating on the largest surface experiencing the tensile and compressive forces than the D orientation. It is also seen that the part of the three-point bend sample

in compression would have more resistance to failure in the T orientation due to the layers being parallel to the force. As the force pushes the sample, the layers, and thus the coating, on the side of the sample in compression, the layers get closer together and the resistance to the force gets higher, which is where the T orientation gets its strength in the three-point bend test. Thus, the A orientation is the strongest followed by the T and then the D orientations.

For the combined orientations, the AD and AT orientations had the highest values in tensile testing while the DT and AT had the highest values in the three-point bending and Izod tests. For the tensile tests, it is desirable to have long continuous layers so that the coating is able to run along the length of the sample. The A orientation achieves this goal, which is the reason that the A orientation is the common orientation between the two strongest combination layer orientations. For the three-point bend test samples, the T orientation adds a resistance to the fracture because the layers are parallel to the force, causing a higher resistance to the force. For the Izod test samples, the T orientation allows for the coating to penetrate further into the sample. This is the reason that the T orientation is the common orientation between the two strongest combination layer orientations. The ADT layer orientation had the shortest layers for the tensile test, the least resistance to fracture for the three-point bend test, and the least amount of penetration for the Izod test, which is the reason that it was consistently the weakest layer combination.

Finally, examining the fracture surface of a tensile sample with a rough coated surface, Fig. 19(a), and comparing it to the smooth coated surface, Fig. 19(b), it can be seen that almost total penetration of the coating on the rough sample was

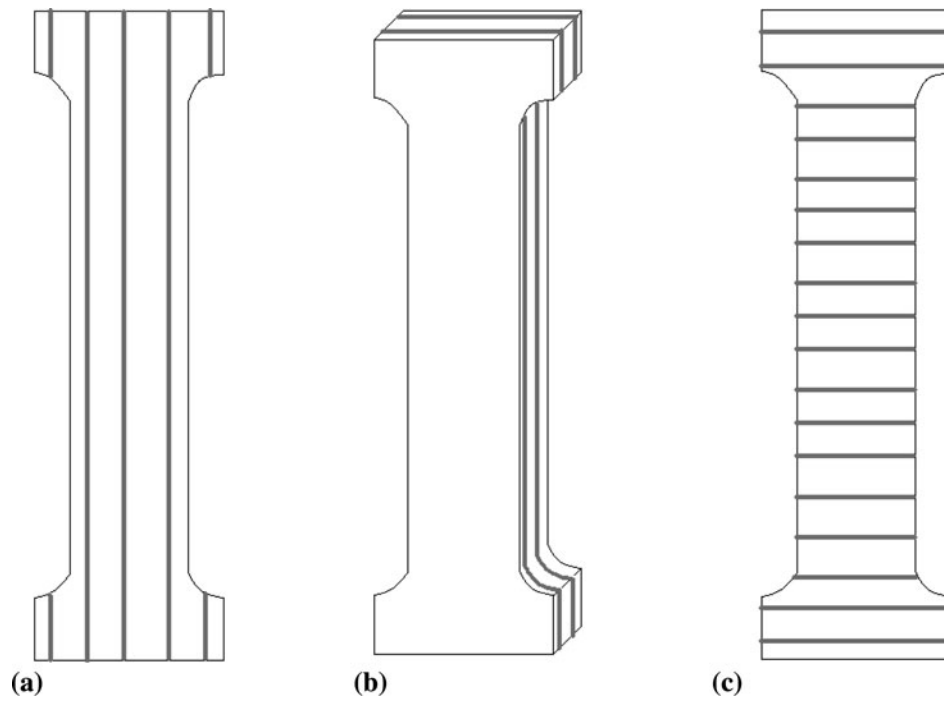


Fig. 16 Schematic of tensile samples showing coating penetration. (a) Crack arrester (A), (b) crack divider (D), and short transverse (T)

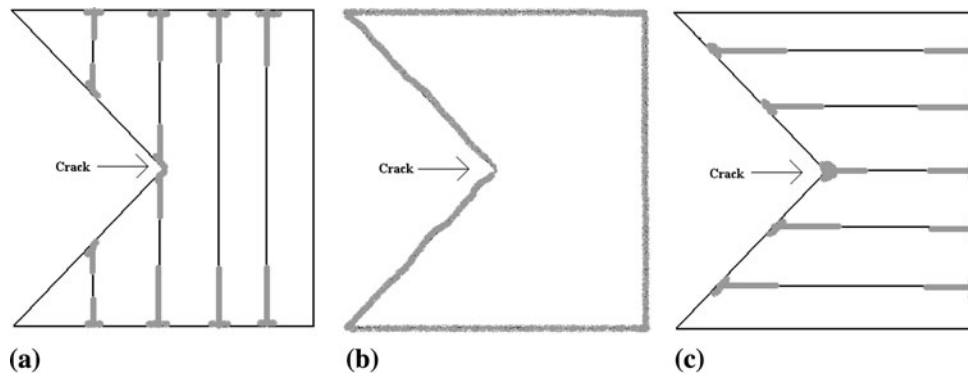


Fig. 17 Cross section profile of impact test samples initial crack showing coating penetration. (a) Crack arrester (A), (b) crack divider (D), and short transverse (T)

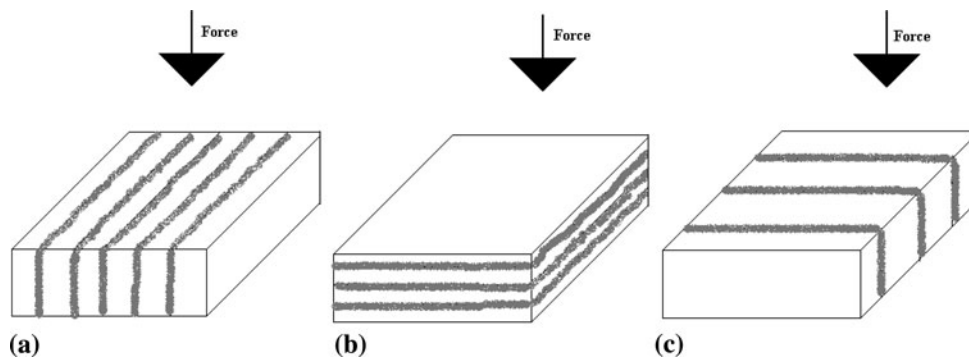


Fig. 18 Schematic of three-point bend samples showing coating penetration. (a) Crack arrester (A), (b) crack divider (D), and short transverse (T)

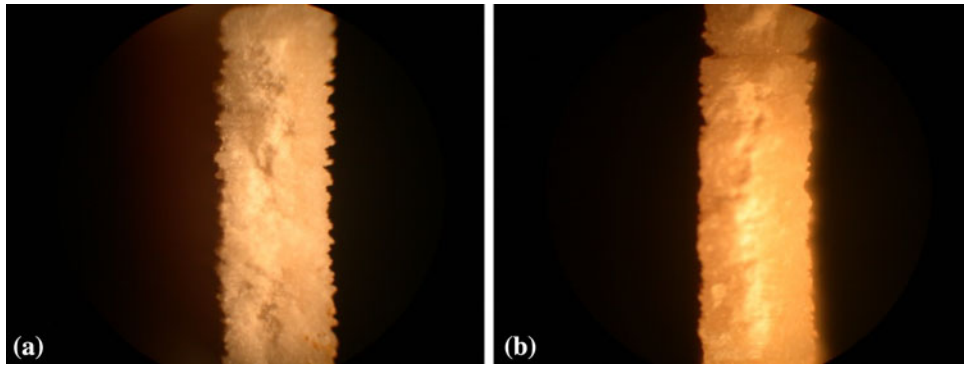


Fig. 19 Tensile test (a) rough sample and (b) smooth sample

obtained whereas on the smooth sample there is more area where the coating never reached.

Another factor not examined in this study is variability of the part. Variability can be introduced in many ways. Some of those ways are the different batches the samples were made of possible impurities in the powder and the actual build orientation within the machine.

5. Summary

The strength and toughness of the samples for this study were determined to a large degree by the coating. The deeper and thicker the coating is, the stronger the sample will be. Surface roughness was also found to play a role in the thickness of the coating. A sample with a very rough surface has many gaps where more coating can penetrate the sample. The rougher the surface is of the sample, the deeper the coating can penetrate, the stronger the final sample will be. The other factor to the thickness and penetration of the coating was the layer orientation. The layer orientation of a sample will either enable or prohibit the penetration of the sample. The coating is allowed to penetrate deeper into the sample when it is moving parallel to the layers of the sample. Very little penetration occurred from layer to layer (through one layer to the next). Special care should be taken when making samples from the RP machine as the level of coating penetration plays an important role in the final strength of the RP sample.

6. Conclusions

1. The A orientation had the highest tensile strength values followed by the D and then the T orientations. This due to the long continuous layers parallel to the length of the sample for the A orientation, making the coating harder to break.
2. The A orientation also had the highest three-point bend test values. It was followed by T and then D. Again, A was highest due to the long continuous layers parallel to the length of the sample. However, the T orientation had higher values than the D orientation due to the resistance of the coating to the force that was parallel to the layer orientation.
3. The A and T orientations had the highest impact energy values followed by the D orientation. This is due to the

penetration of the coating. The A and T orientations allowed for deeper penetration of the coating along the axis of the force, whereas the D orientation had minimal penetration at the same axis. However, the variation in the Weibull analysis for the D orientation was much smaller than that in the A and T orientations.

4. The AT and AD orientations were the strongest combination orientations for the tensile test. This is because the A orientation combined with the D and the T orientation allows for the sample to have long layers running parallel to the length of the sample with a deeper penetration of the coating than the other layer orientation combinations.
5. The AT and DT orientations had the highest three-point bend test values and highest impact energies. This is because the T orientation for these two tests allowed for a resistance to the force that was parallel to the layers of the samples for the three-point bend test and for a deeper penetration of the coating in the Izod tests. Combining the T orientation with the A and the D orientation is the reason that these orientations had higher strength and toughness values.
6. The ADT orientation was the weakest layer orientation combination because it had the shortest layers for the tensile test, the least resistance to fracture for the three-point bend test, and the least amount of penetration for the Izod test.
7. The coating obscured the imaging of the orientation of the layers.
8. The penetration of the coating significantly determined the strength and toughness values of the samples.
9. The roughness of the surfaces determined the thickness of the coating.

Acknowledgment

The authors are grateful to Dr. R. Noorani of the mechanical engineering department at Loyola Marymount University for allowing them to use the Rapid Prototype equipment.

References

1. Z Corporation: Material Safety Data Sheet, "ZP™ 130 Powder," April 2005
2. Z Corporation: Material Safety Data Sheet, "ZP™ 58 Binder," June 2005

3. Technology Supplies Ltd: Material Safety Data Sheet, MSDS No.: 0005. "Z-Bond™ 101 Medium Strength Cryanoacrylate," 8 August 2005
4. J.D. Embury, N.J. Petch, A.E. Wraith, and E.S. Wright, The Fracture of Mild Steel Laminates, *Trans. Metall. Soc. AIME*, 1967, **239**, p 114–118
5. O.S. Es-Said, J. Foyos, R. Noorani, M. Mendelson, and R. Marloth, Effect of Layer Orientation on Mechanical Properties of Rapid Prototyped Samples, *Mater. Manuf. Process.*, 2000, **15**(1), p 107–122
6. Spectrum Z510 Users Manual, http://www.ems-usa.com/pdf/EMS_Z510_brochure.pdf, 2009
7. Y. Xu, L. Cheng, L. Zhang, D. Yan, and C. You, Optimization of Sample Number for Weibull Function of Brittle Materials Strength, [www.sciencedirect](http://www.sciencedirect.com)